Supporting Information

Dual-Channel Logic Gates Operating on the Chemopalette ssDNA-Ag NCs/GO Nanocomposites

Da-Qian Feng and Guoliang Liu*

School of Chemistry and Chemical Engineering, Yancheng Institute of Technology, Yancheng 224051, China.

*To whom correspondence should be addressed. Fax/Tel: +86-515-88298190. E-mail: liuguoliang199@126.com; glliu@ycit.edu.cn.

Contents

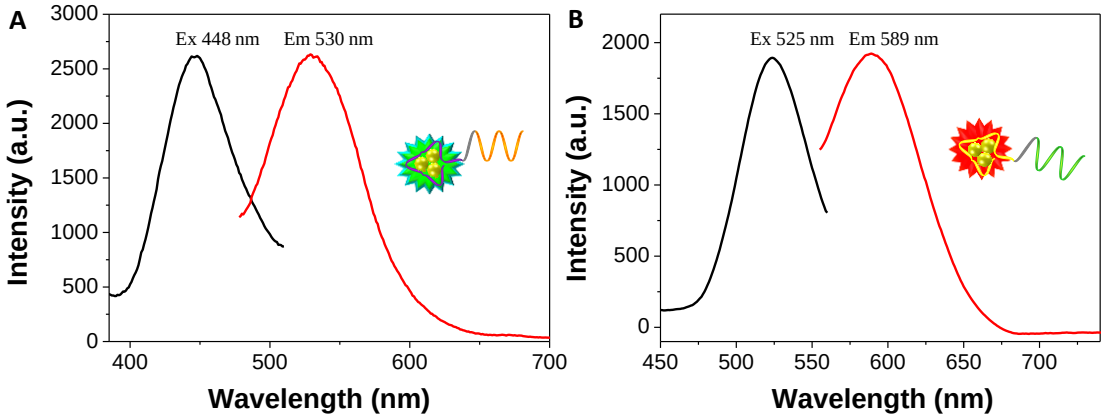

Figure S1. (A) The fluorescent excitation (black line) and emission (red line) spectra of synthesized G-Ag NCs-CH5N1 stabilized by the nucleic acid sequence **1**. (B) The fluorescent excitation (black line) and emission (red line) spectra of synthesized R-Ag NCs-CH1N1 stabilized by the nucleic acid sequence **2**.

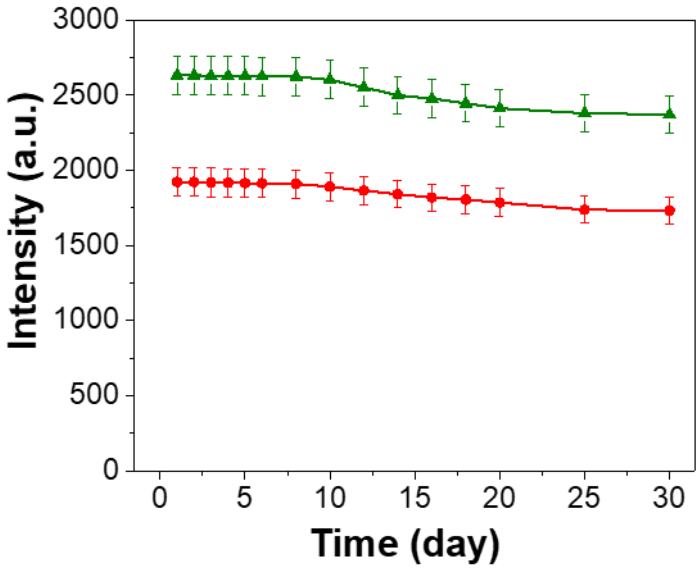

Figure S2. The investigation on the stability of fluorescent silver nanoclusters G-Ag NCs-CH5N1(green curve) at 530 nm and R-Ag NCs-CH1N1(red curve) at 589 nm. The fluorescence spectra were measured for three parallel tests when the solutions had been stored at 4 ℃ for corresponding time.

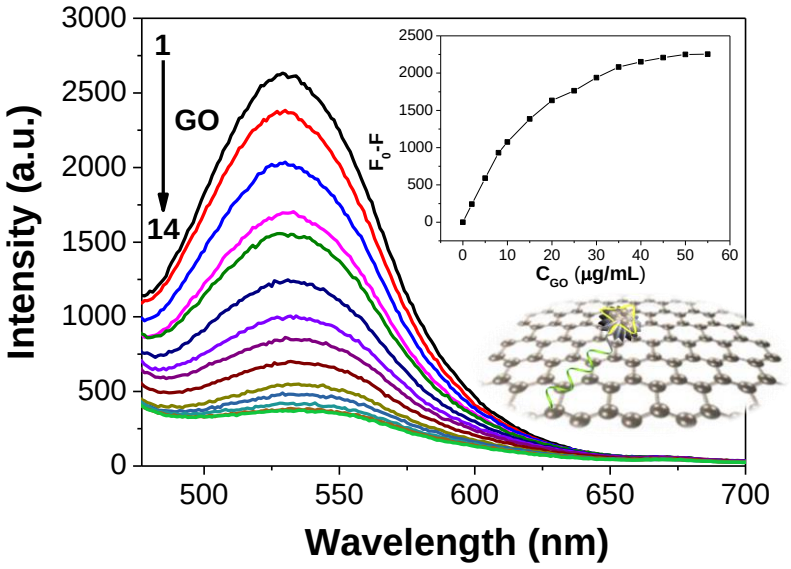

Figure S3. Effects of GO concentration on the fluorescence responses of the G-Ag NCs-CH5N1/GO nanocomposites. The fluorescence spectra of G-Ag NCs-CH5N1 in the presence of different amounts of GO from 0 to 55 μg/mL. Conditions: 1, G-Ag NCs-CH5N1; 2–14: 1 + GO (μg/mL): 2, 5, 8, 10, 15, 20, 25, 30, 35, 40, 45, 50, and 55. The inserted figure is the curve of fluorescence intensity change (F_0-F) of the G-Ag NCs-CH5N1/GO solution at 530 nm versus the concentration of GO from 0 to 55 μg/mL.

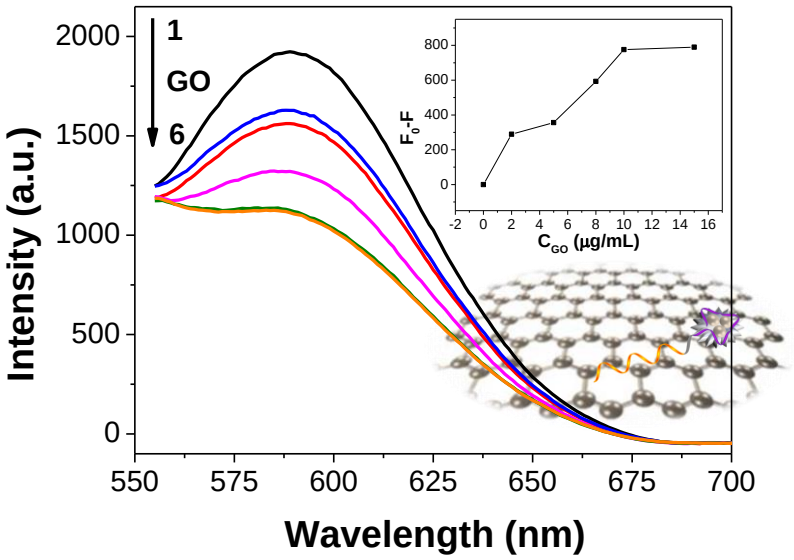

Figure S4. Effects of GO concentration on the fluorescence responses of the R-Ag NCs-CH1N1/GO nanocomposites. The fluorescence spectra of R-Ag NCs-CH1N1 in the presence of different amounts of GO from 0 to 15 μg/mL. Conditions: 1, R-Ag NCs-CH1N1; 2–6: 1 + GO (μg/mL): 2, 5, 8, 10, and 15. The inserted figure is the curve of fluorescence intensity change (F_0-F) of the R-Ag NCs-CH1N1/GO solution at 586 nm versus the concentration of GO from 0 to 15 μg/mL.

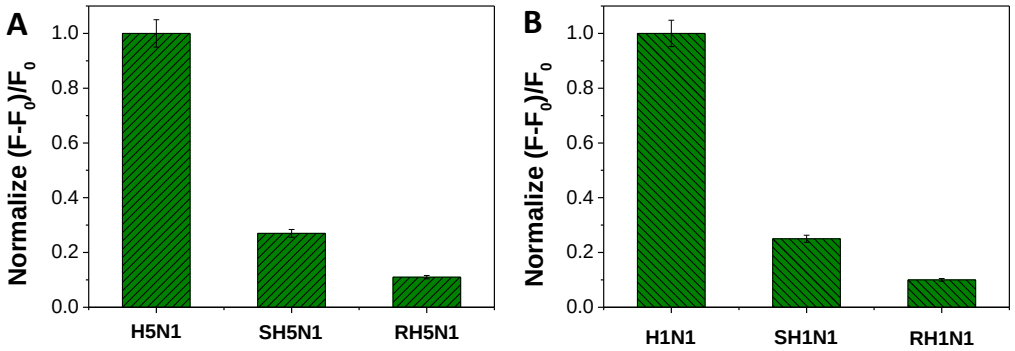

Figure S5. (A) The histogram of the fluorescence enhancement $(F-F_0)/F_0$ of the G-Ag NCs-CH5N1/GO nanocomposites in the presence of target DNA (H5N1, sequence **3**), single-base mismatch DNA (SH5N1, sequence **7**), and random DNA (RH5N1, sequence **8**). (B) The histogram of the fluorescence enhancement $(F-F_0)/F_0$ of the R-Ag NCs-CH1N1/GO nanocomposites in the presence of target DNA (H1N1, sequence **4**), single-base mismatch DNA (SH1N1, sequence **9**), and random DNA (RH1N1, sequence **10**). F_0 and F correspond to the fluorescence intensity of the G-Ag NCs-CH5N1/GO or R-Ag NCs-CH1N1/GO nanocomposites system in the absence and presence of target DNAs, respectively. Error bars were obtained from three parallel experiments.

Table S1. Compared fluorescent recovery rate calculated in this study with the reported other assays.

Probes	Sequences (5'-3')	Em (nm)	Fluorescent recovery rate	References
9 ASNCB	**CCCTTTAACCCCTTCTTCATCGAGAGTGTAGTCGGAAGAA-BHQ1**	520	209%	15
15 ASNCB	**CCCTTTAACCCCTAGGTTGGTGTGGTTGGTGTGGTTGGACACCAACC-BHQ1**	546	51.1%	15
R-Ag NCs-CH1N1	**CCTCCTTCCTCCTTCTTCATCGAGAGTGTAGTCG**	589	200%	This study

Table S2. The truth table of the INHIBIT logic gate for H5N1 gene detection based on G-Ag NCs-CH5N1/GO nanocomposites.

Input 1 (H5N1)	Input 2 (CH5N1)	Output
0	0	0
1	0	1
0	1	0
1	1	0

Table S3. The truth table of the INHIBIT logic gate for H1N1 gene detection based on R-Ag NCs-CH1N1/GO nanocomposites.

Input 1 (H1N1)	Input 2 (CH1N1)	Output
0	0	0
1	0	1
0	1	0
1	1	0

Nos	Input 1 (H1N1)	Input 2 (H5N1)	Input 3 (CH1N1)	Input 4 (CH5N1)	Output	Judgment
a1	0	0	0	0	0	No target
a2	0	0	1	0	0	
a3	0	0	0	1	0	
b1	1	0	0	0	1 (orange)	H1N1
b2	1	0	1	0	0	
b3	1	0	0	1	1 (orange)	
c1	0	1	0	0	1 (yellow-green)	H5N1
c2	0	1	0	1	0	
c3	0	1	1	0	1 (yellow-green)	
d1	1	1	0	0	1 (yellow)	H1N1/H5N1
d2	1	1	1	0	1 (yellow-green)	
d3	1	1	0	1	1 (orange)	
d4	1	1	1	1	0	

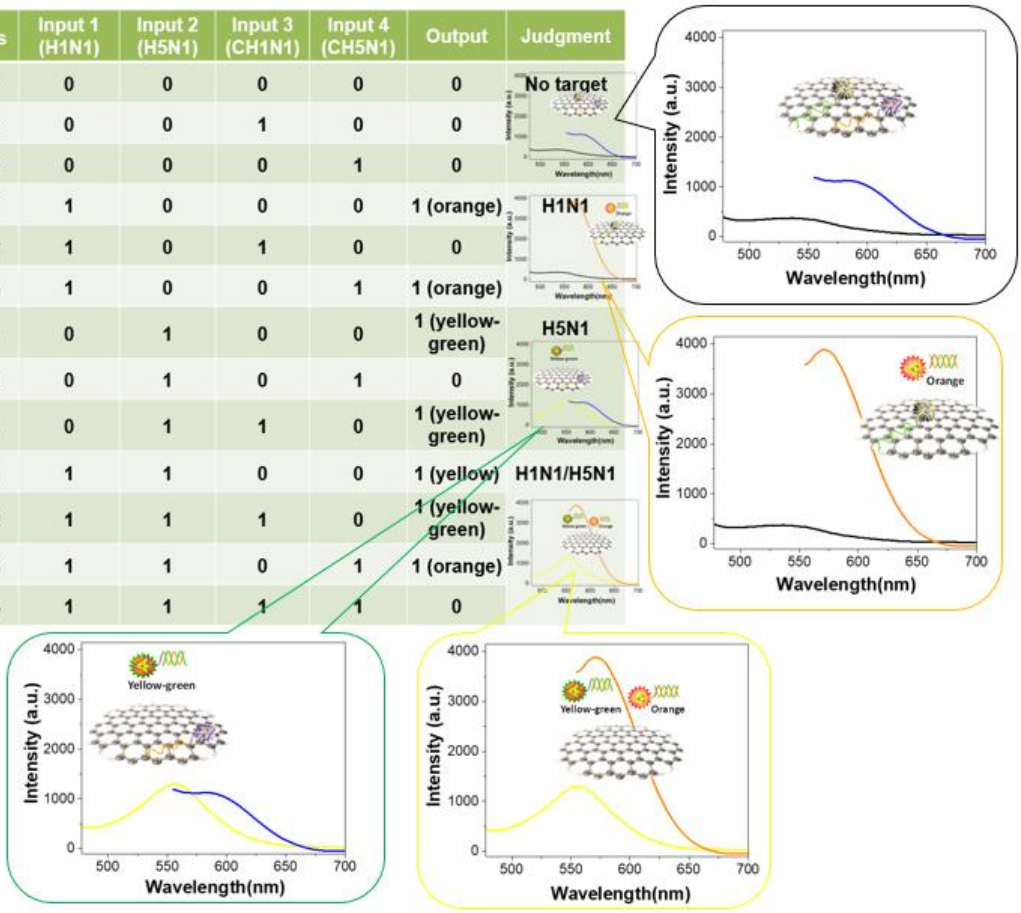

Figure S6. Truth table of combinatorial logic gates for the multiplexed detection of H1N1 and H5N1 based on ssDNA-Ag NCs conjugating the complementary sequence of target virus subtype genes/GO nanocomposites.

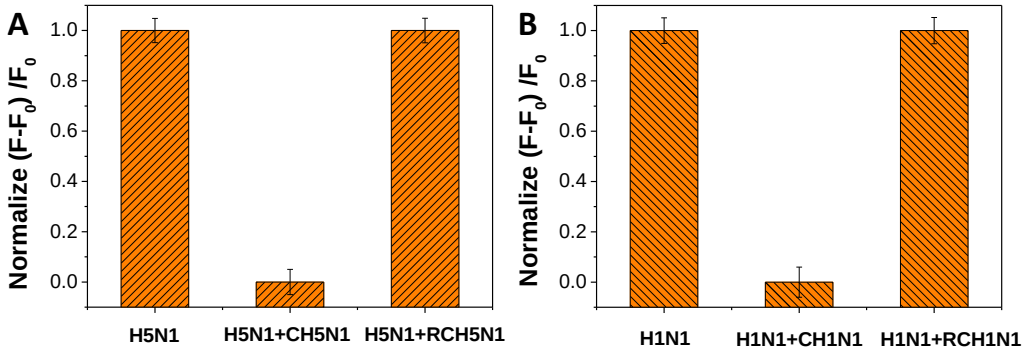

Figure S7. (A) The histogram of the fluorescence enhancement $(F-F_0)/F_0$ of the G-Ag NCs-CH5N1/GO nanocomposites in the presence of target DNA (H5N1, sequence **3**), H5N1 + the complement sequence of target virus gene (CH5N1, sequence **5**), and H5N1 + the random sequence of the complement sequence of target virus gene (RCH5N1, sequence **11**). (B) The histogram of the fluorescence enhancement $(F-F_0)/F_0$ of the R-Ag NCs-CH1N1/GO nanocomposites in the presence of target DNA (H1N1, sequence **4**), H1N1 + the complement sequence of target virus gene (CH1N1, sequence **6**), and H1N1 + the random sequence of the complement sequence of target virus gene (RCH1N1, sequence **12**). F_0 and F correspond to the fluorescence intensity of the G-Ag NCs-CH5N1/GO or R-Ag NCs-CH1N1/GO nanocomposites system in the absence and presence of target DNAs, respectively. Error bars were obtained from three parallel experiments.

Table S4. Summary of the reported fluorescence DNA sensing methods.

Method	Detection limit (nM)	Detection time interval (h)	References
Activatable SNCB	2	0.5	16
GO/molecular beacons	2	2	30
GO/nucleic-acid-stabilized Ag NCs	0.5	1-1.5	31
DNA-templated Ag NCs	25	24	38
Polymerization/nicking DNA machine	1-10	4-10	39
Releasing acridine orange from GO	50	-	40
Cobalt oxyhydroxide nanoflake	0.5	0.25	41
Chemopalette ssDNA-Ag NCs/GO	0.1 or 1	0.33	Present study